

The effects of Hurricane Harvey on Texas coastal zone chemistry

Piers Chapman^{1,2}, Steven F. DiMarco^{1,2}, Anthony H. Knap^{1,2}, Antonietta Quigg^{1,3}, Nan D. Walker⁴

1. Department of Oceanography, Texas A&M University, College Station, TX 77843, USA

2. Geochemical and Environmental Research Group, Texas A&M University, College Station, TX 77843, USA

3. Department of Marine Biology, Texas A&M University, Galveston, TX 77553, USA

4. Department of Oceanography and Coastal Sciences, Louisiana State University, Baton Rouge, LA, 70803, USA

Correspondence to: Piers Chapman (piers.chapman@tamu.edu)

Abstract

Hurricane Harvey deposited over 90 billion cubic meters of rainwater over central Texas, USA, during late August/early September 2017. During four cruises (June, August, September and November 2017) we observed changes in hydrography, nutrient and oxygen concentrations in Texas coastal waters. Despite intense terrestrial runoff, nutrient supply to the coastal ocean was transient, with little phytoplankton growth observed and no hypoxia. Observations suggest this was probably related to the retention of nutrients in the coastal bays, rapid uptake by phytoplankton of nutrients washed out of the bays, as well as dilution by the sheer volume of rainwater, and the lack of significant carbon reserves in the sediments, despite the imposition of a strong pycnocline. By the November cruise conditions had apparently returned to normal and no long-term effects were observed.

Keywords

Hurricane Harvey, Texas coast, nutrients, oxygen, chlorophyll

1. Introduction

The Gulf of Mexico is renowned for its hurricanes and tropical storms, and 2017 was a very active year in the Atlantic, with 10 hurricanes and 8 tropical cyclones and depressions. Hurricane Harvey developed in the Bay of Campeche, in the extreme southwest of the Gulf of Mexico, on 23 August, 2017, intensifying rapidly on 24 August over water with SST $>30^{\circ}$ C and an upper ocean heat content anomaly (measured by three ARGOS floats) that extended to ~ 45 m water depth (Trenberth et al., 2018). Harvey crossed the edge of the Texas shelf in the northwestern Gulf at 18.00 U.S. Central Time having intensified to category 3, and reached category 4 strength by midnight of 25 August with sustained wind speeds of 60 m s^{-1} (115 kt) and a minimum central pressure of 937 mbar (Blake and Zelinsky 2018). Rapid intensification of tropical cyclones over the shallow waters of the south Texas shelf has been reported previously and is believed to be related to periods when warm water occupies the whole water column. This prevents mixing of colder bottom water that can reduce the energy flux feeding the hurricane (Potter et al., 2019). The storm came ashore near Corpus Christi, TX on 26 August, and stalled over the TX coast, moving slowly to the northeast until August 31, after which it moved inland and dissipated over Kentucky (Fig. 1).

Harvey brought a storm surge of up to 3 m and widespread torrential rain to the Texas coast, with the heaviest rainfall, over 1500 mm (60 in), measured at Nederland and Groves, near Houston (Blake and Zelinsky, 2018). Heavy rain (<500 mm) also affected Louisiana (Fig.1). This unprecedented rainfall, the highest ever recorded in the U.S. for a tropical cyclone, resulted in widespread flooding in Texas and Louisiana (Emanuel, 2017; Balaguru et al., 2018). It is estimated that the total volume of rainfall over Texas and Louisiana during Harvey's passage was between $92.7 \times 10^9 \text{ m}^3$ (Fritz and Samenow, 2017), and $133 \times 10^9 \text{ m}^3$ (DiMarco, unpublished), and over 200 mm of rain was recorded as far inland as Tennessee and Kentucky as the storm died down (Blake and Zelinski, 2018; Fig.1). In addition to the rain that fell on land, DiMarco (unpublished) has estimated that about another $44 \times 10^9 \text{ m}^3$ fell over the ocean.

Fig 1

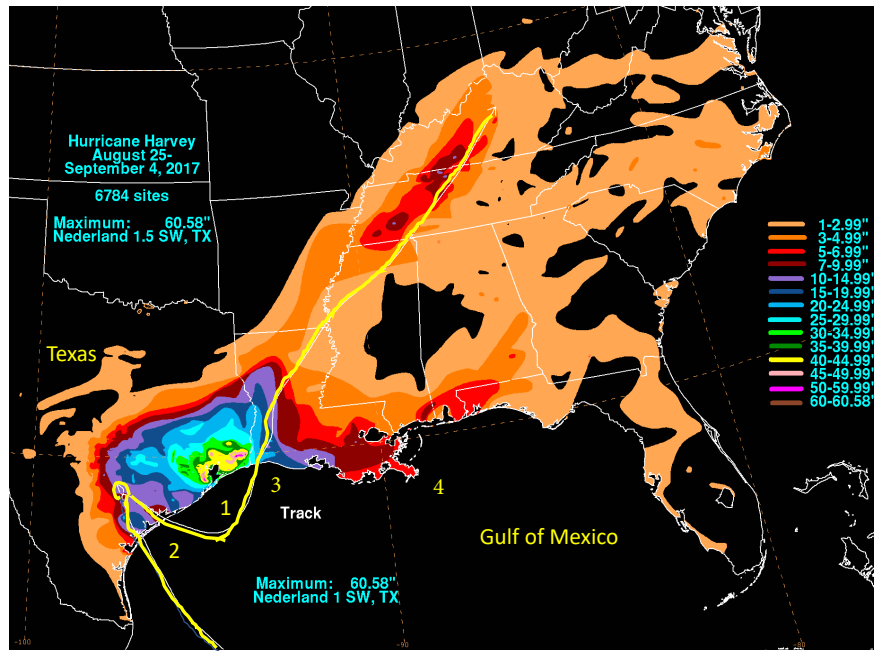


Fig. 1. Track of Hurricane Harvey and associated rainfall (in inches) over the southern United States, 24 August-4 September, 2017 (from Blake and Zelinsky, 2018, with permission from NOAA). The numbers 1, 2 and 3 denote the positions of Galveston Bay, Matagorda Bay, and Lake Sabine respectively. The Mississippi delta (in Louisiana) is shown as 4. The Nederland 1.5 SW rain gauge, which recorded the highest rainfall, is at 29.95°N, 94.01°W.

Galveston Bay collects the runoff from the Houston metropolitan region. Following the storm, the bay became a freshwater lake (Du et al., 2019; Steichen et al., 2020; Thyng et al., 2020) as it was flushed with about three to five times its volume of rainwater. U.S. Geological Survey (USGS) data (downloaded from <https://waterdata.usgs.gov> on 25 June 2020; all such records are collected in cubic feet per second (cfs) and have been converted to $\text{m}^3 \text{s}^{-1}$) show very rapid increases in flow rates in Texas rivers and streams following the storm's landfall. For instance, flows in the Colorado and Brazos Rivers south of Galveston Bay (USGS stations 08162000 and 08111500 respectively; Figs S1a and S1b) increased from $<2,000$ cfs ($\sim 60 \text{ m}^3 \text{s}^{-1}$) during most of August to over 90,000 cfs ($>2,500 \text{ m}^3 \text{s}^{-1}$) by the beginning of September, while flow in the San Jacinto River (USGS station 08068090, Fig. S1c) and the Trinity River at Liberty (USGS station 08067000, Fig. S1d), which both flow into Galveston Bay, exceeded 100,000 cfs ($3,400 \text{ m}^3 \text{s}^{-1}$). The gauge at Liberty was unfortunately not operational immediately prior to 27 August or after 9 September, but during June flowrates were typically 10,000 – 14,000 cfs ($\sim 300\text{--}420 \text{ m}^3 \text{s}^{-1}$). Such

large changes in runoff are known to produce major changes in estuaries and coastal waters (e.g., Ahn et al., 2005; Paerl et al., 2001, 2006; Mallin and Corbett, 2006; De Carlo et al., 2007; Zhang et al., 2009; Du et al., 2019; Thyng et al., 2020). Liu et al. (2019) and Steichen et al. (2020) reported changes in the phytoplankton community within Galveston Bay as the salinity decreased and then increased again.

The massive runoff led to turbidity plumes visible well offshore (Fig. S2). D'Sa et al. (2018) monitored large increases in terrestrial carbon (25.22×10^6 kg) and suspended sediments (314.7×10^6 kg) entering Galveston Bay during the period 26 August-4 September. The plume off Galveston Bay on 31 August extended at least 55 km offshore (Du et al., 2019), and surface water with a salinity of 15 was measured on 1 September at the Texas Automated Buoy System (TABS) buoy F (28.84°N, 94.24°W; yellow diamond in Fig. S2), where it is typically 31-32 (data from <https://tabs.gerg.tamu.edu>, downloaded on 6 June 2018). Normal salinities did not return until 8 September. Similar sediment plumes at the mouths of the Brazos and Guadalupe estuaries can be seen in Fig. S2, and such plumes and lowered salinities have been reported from the Lavaca-Colorado and Nueces-Corpus estuaries near Corpus Christi (Walker et al., 2021). It is likely that other bays and estuaries along the Texas coast were similarly affected, as they were all under the path of the hurricane.

We report here on data collected before and after the hurricane along the Texas coast between Galveston and Padre Island, south of Corpus Christi, Texas. Two cruises were completed prior to the hurricane as part of a separate project. Following the hurricane, we completed three more cruises, occupying the same stations in September (twice) and November 2017. This paper reports on the changes in the water column between the pre- and post-hurricane cruises as they relate to stratification, nutrient supply and oxygen concentrations.

2. Methods

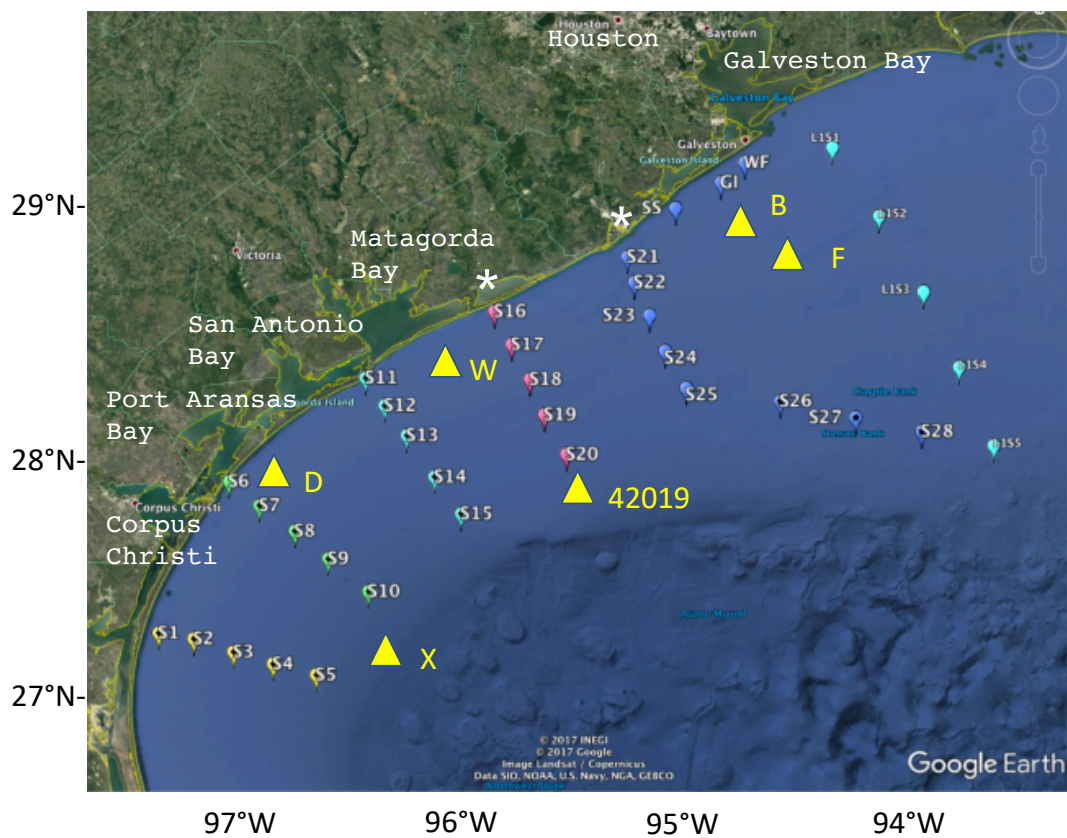
Pre-hurricane cruises on the R.V. *Manta* took place from 12-16 June and 7-11 August 2017, while post-hurricane cruises were from 22-27 September, 29 September – 1 October, and 15-20 November on the R.V. *Point Sur*. The 27 September-1 October cruise only occupied the two inshore stations on each line; all other cruises covered a standard grid of five lines of five

stations each (Fig. 2), together with supplemental *ad hoc* stations between lines and offshore in the east of the region towards the Flower Gardens Banks National Marine Sanctuary, a shallow reef system 120 km south of Galveston Bay near 27.92°N, 93.75°W. During the November cruise, stations were added at the outer ends of the southernmost lines to ensure sampling of offshore surface water with salinity >35. Depths at the outer ends of each line decreased from 95-110 m at stations 5 and 10 to 85 m at station 15, and 50 m at stations 20 and 25.

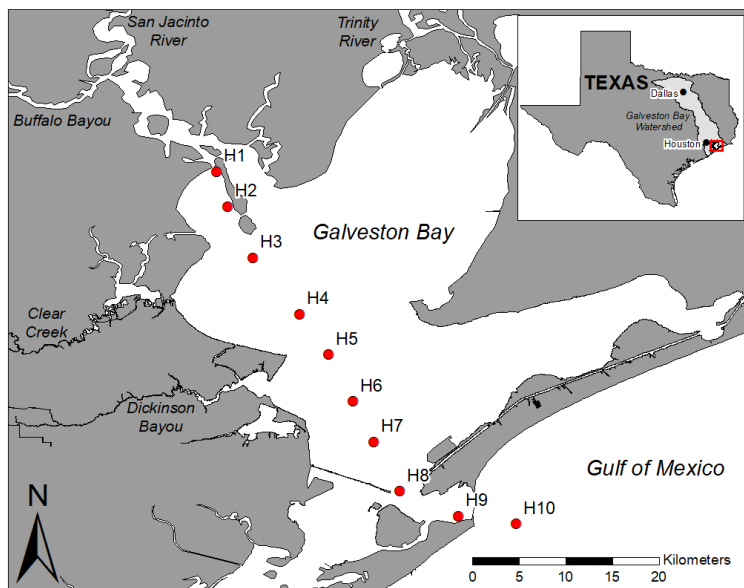
At each station, a full-depth CTD cast was made using a SeaBird 911 CTD fitted with a SBE-55 temperature sensor, SBE-3 conductivity sensor, SBE-45 pressure sensor, and a SBE-43 oxygen probe. Additional sensors on the rosette package included a Chelsea Instruments Aqua3 fluorometer and a Biosperical/Licor PAR sensor. Discrete samples were collected from a 6-bottle rosette for salinity determinations ashore (± 0.002) and for oxygen calibration ($\pm 0.3 \mu\text{mol/L}$, by Winkler titration on board ship). Nutrient samples were collected, filtered, frozen on board and analyzed ashore for nitrate, nitrite, phosphate, silicate, and ammonia by standard autoanalyzer methods (WHPO 1994). Limits of detection (and precision) are about $0.1 \mu\text{mol/L}$ for nitrate (2%), silicate (1%) and ammonia (3%), and $0.02 \mu\text{mol/L}$ for nitrite (1%) and phosphate (2%). Local meteorological data were collected by the ship's system, while surface water temperature and salinity data came from the ships' flow-through system.

Wind and current data are available from the TABS moorings along the Texas coast (see Fig. 2 for positions and <http://tabs.gerg.tamu.edu> for the data archive). Buoy B (off Galveston) provided both wind and current data from before Harvey's landfall with a gap in the first half of August; buoys W (off Matagorda Bay) and D (off Corpus Christi) provided current data only. We have used additional wind data from TABS buoy X, which provided data until it failed on the morning of 25 September, and NOAA buoy 42019 (29.91°N, 95.34°W, obtained from the National Data Buoy Center at <https://www.ndbc.noaa.gov>, downloaded 7 July 2020).

Fluorometer data were obtained at each station sampled using a Chelsea Aqua 3 instrument on the rosette. This instrument was calibrated prior to and after the cruises, but not immediately. Satellite imagery (Aqua-1 MODIS sensor, Level 2 Ocean Color files) downloaded from the NASA Goddard ocean color website (<https://oceancolor.gsfc.nasa.gov>, downloaded 25 May



140



141

Fig. 2. Stations occupied during the four cruises. Only stations S1-S25 and the inshore stations GI, SS and WF were occupied during June and August. All stations shown were occupied in the 22-27 September cruise and in November. Only the two inshore stations on each line were occupied during the second September cruise. Yellow triangles show positions of TABS moorings B, D, F, W and X, and NOAA buoy 42019. White stars show the mouths of the Colorado River (near station 16) and Brazos River (near station 21). Data from stations 11-15 are shown in Figs. 5, 6 and supplementary figures. (b) Galveston Bay and vicinity showing Trinity and San Jacinto rivers and stations discussed in Fig. 8.

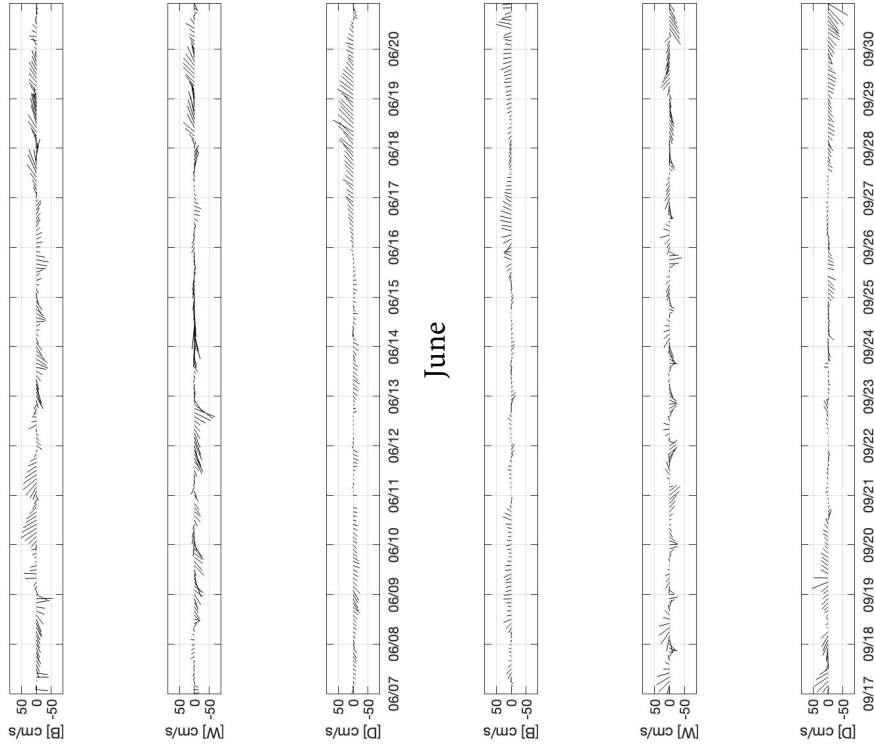
2019) were processed using the NASA SeaDAS software. In reality, the satellite-derived values may be too high, due to the presence of CDOM after the storm (D'Sa et al., 2018), as the OC3 algorithm provided by the SeaDAS software cannot discriminate between chlorophyll *a* and CDOM.

3. Results

3.1 Wind fields

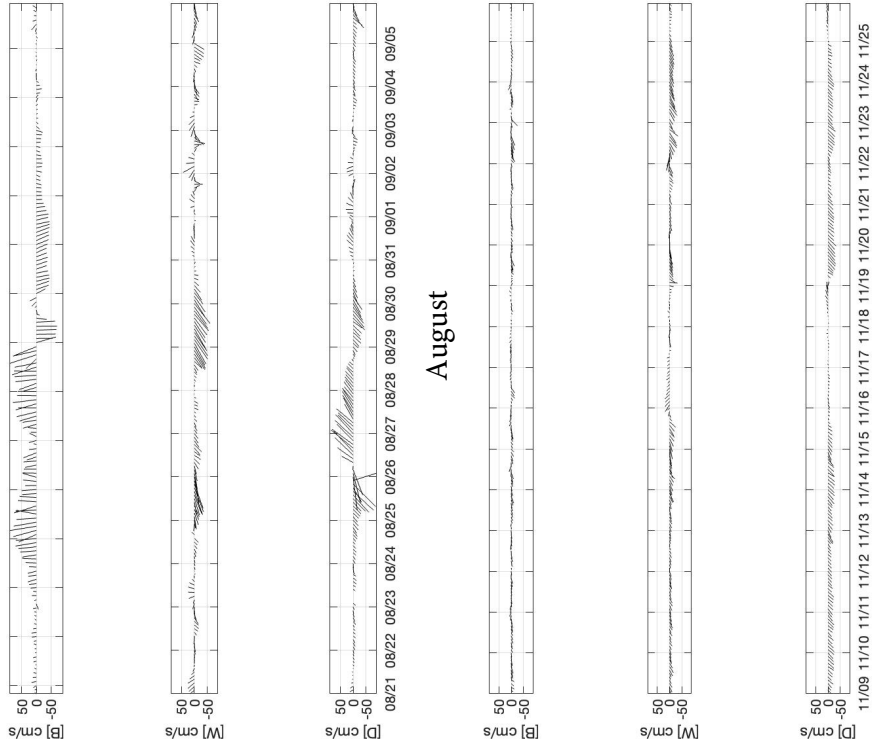
Wind data from all moorings (not shown) were typical of summer conditions in this part of the Gulf of Mexico, being predominantly from the south with occasional reversals (Nowlin et al., 1998). At TABS buoy B, wind velocities during June and July were generally 5-8 m s⁻¹ and varied between SSE and SSW. Following a gap in data from 31 July until 22 August, they remained in this quadrant until the passage of the hurricane, although wind speeds increased from 3-4 m s⁻¹ on 22 August to 12 m s⁻¹ on 29 August when they were from the north. After the hurricane, September winds again were predominantly from the SE/SSE, with the exception of two short-lived reversals on 5 and 10-12 September, with wind speeds around 4-7 m s⁻¹.

Further south and offshore, at TABS mooring X and NOAA mooring 42019, weak northerly winds (generally <4 m s⁻¹) occurred from 6-8 June, with a second northerly spell from 20-22 June, when speeds reached 10 m s⁻¹ at mooring X and 15 m s⁻¹ at 42019. After this second frontal system, winds reverted to SE/SSE at both moorings until the passage of Hurricane Harvey at the end of August. During September, at mooring 42019, winds were primarily from the NNE/ENE at 4-10 m s⁻¹ until the 12th, and again from the 27th, with SE or easterly winds of 3-7 m s⁻¹ from 14-26 September. Maximum sustained wind speeds recorded during the hurricane at this mooring were 17 m s⁻¹, with gusts to 22.6 m s⁻¹. During October, there were two northerly/



June

September



August

November

Fig. 3. Current vectors at TABS buoys B, D and W during the cruise in June, the period of the hurricane (August), and the cruises in September and November.

westerly wind events, on the 16th, when winds reached speeds of 15 m s^{-1} , and a sustained event from 25-28 October, again with speeds $< 15 \text{ m s}^{-1}$. Northerly winds continued during November, with sustained winds of $12\text{-}14 \text{ m s}^{-1}$ during the periods 8-11, 18-20, and 22-24.

3.1 Water movement

Water movement over the Texas shelf is typically downcoast (towards the southwest) in non-summer months and upcoast (towards the northeast) in summer, with currents following the wind (Cochrane and Kelly, 1986; Walker, 2005). Upcoast winds and currents promote upwelling and act to retain water from the Mississippi-Atchafalaya system on the east Texas-Louisiana shelf (Hetland and DiMarco, 2008), while downcoast flow is downwelling-favorable and can reduce local stratification. During June 2017, currents at Buoy D (27.96° N , 96.84° W) were essentially downcoast from prior to the cruise until 15 June, when they switched to upcoast until 20 June, after which they flowed downcoast again (Fig. 3a). The current reversal took place slightly later (17 June) at Buoys B (28.98° N , 94.90° W) and W (28.35° N , 96.02° W), but the return to downcoast flow again occurred on 20 June at both sites (Fig. 3a). These three moorings are all situated close to the coast in water depths of $20 \pm 2 \text{ m}$.

Upcoast currents prevailed at sites W and D during the August cruise (Fig. 3), although currents were downcoast from about 8-10 August at W and 9-11 August at site D (not shown). Buoy B did not record current speeds during this period, but was back in service immediately before the hurricane arrived. During the passage of the hurricane, the southernmost mooring (buoy D) recorded strong currents of $> 1 \text{ m/s}$ which changed from downcoast to upcoast and back to downcoast again as the storm moved towards the northeast (Fig. 3b). Buoy W recorded continuous downcoast currents during the period of the hurricane, while buoy B showed strong onshore currents ($< 1.0 \text{ m s}^{-1}$) until 30 August, when currents reversed to offshore at $< 80 \text{ cm s}^{-1}$. Following the hurricane, coastal currents were considerably weaker at all three sites in September and November. During the September cruise there were a number of current reversals, especially at buoy W, although velocities were generally $< 30 \text{ cm s}^{-1}$ (Fig. 3c). By

November, current velocities decreased still further and the expected flow towards the west was reinstated (Fig. 3d).

3.2 Temperature, precipitation and salinity

Temperatures (not shown) showed well-mixed or weakly stratified water inshore in June and August with surface-bottom differences of less than 2°C at the two inshore stations on each line. Further offshore, bottom temperatures decreased with depth but there remained a well-mixed surface layer of 15-25m thickness. Following the hurricane, however, the mixed layer extended offshore to the third station on each line in September and almost all stations in November, when isothermal water was found as deep as 80m in some instances, and bottom temperatures were often warmer than at the surface.

Surface temperatures increased from about 28.5 °C in June to over 30 °C in August (Trenberth et al., 2018). As the hurricane passed, temperatures at the buoys, including at NBDC buoy 42019 (27.91° N, 95.34° W), decreased to a minimum of about 27.5 °C, but recovered to 28.5-29 °C by the September cruises. By November, temperatures had decreased to 21-22 °C, 22-23 °C and 23-23.5 °C at buoys B, W and D respectively. NBDC buoy 42019, which is further offshore in 82 m of water, registered temperatures between 25.4° and 26.0°C during this period.

Precipitation measurements for a number of stations in central Texas is shown in Table 1. With the exception of the August data, all stations reported lower than average rainfall during these months apart from Houston Intercontinental Airport in June and July, and Austin International Airport in September (respectively north and northwest of Galveston Bay). Despite this, low salinities were found in June at the surface inshore and pushing southwards (Fig. 4a), with a strong, sloping salinity front between the surface layer and the deeper water. Salinity values across the front changed by ~12 along stations 18-20 and 21-23 just south of Galveston Bay. The salinity gradient decreased towards the south, with an inshore-offshore change of only 4 south of 28°N. The lowest surface salinity (station 21) was <22 at this time, and was still <32 along the southernmost line except at the outermost station. Bottom water salinities (not shown) were higher because of density stratification, with salinities of >35 found in water deeper than about 20m at stations in the eastern half of the grid and 35 m on the southern lines. The low surface

Table 1. Precipitation (cm) for sites in central Texas from May-September 2017 compared with the long-term mean (italics). Data downloaded from https://www.srcc.tamu.edu/climate_data_portal/?product=precip_summary (accessed 7.07.2021).

	May	June	July	Aug	Sept
Austin International airport (30.20°N, 97.66°W)	7.59 <i>11.86</i>	6.17 <i>8.28</i>	2.69 <i>4.65</i>	32.99 <i>6.20</i>	9.68 <i>8.46</i>
Corpus Christi airport (27.77°N, 97.50°W)	8.18 <i>8.51</i>	4.90 <i>8.00</i>	3.22 <i>5.97</i>	14.98 <i>7.87</i>	3.71 <i>13.41</i>
Houston Hobby airport (29.65°N, 95.28°W)	6.81 <i>12.80</i>	13.20 <i>13.84</i>	7.92 <i>11.40</i>	98.73 <i>11.81</i>	9.52 <i>13.13</i>
Houston Intercontinental airport (29.99°N, 95.34°W)	6.12 <i>13.59</i>	18.26 <i>14.22</i>	15.98 <i>9.45</i>	99.34 <i>11.10</i>	3.12 <i>12.09</i>
San Antonio airport (29.53°N, 98.46°W)	4.48 <i>10.18</i>	1.02 <i>8.58</i>	0.41 <i>5.92</i>	14.91 <i>6.12</i>	7.11 <i>9.32</i>
Victoria airport (28.84°N, 96.92°W)	7.77 <i>12.85</i>	8.92 <i>11.10</i>	0.94 <i>8.25</i>	43.03 <i>7.82</i>	7.92 <i>12.52</i>

salinities resulted from westward flow from the Mississippi-Atchafalaya river system (MARS), together with local outflow from Galveston Bay. MARS peak flow during the 2017 spring flood was 34,500 m³ s⁻¹, almost double the long-term mean from 1935-2017 (data from <http://rivergages.mvr.usace.army.mil/>, accessed 7 July 2021).

By August (Fig.4b), surface salinities had increased across the region as a result of the southerly winds, with a minimum of 32.15 just south of Galveston Bay, while the 35 surface isohaline was situated off Matagorda Bay between stations 16-20 and 11-15. Bottom water was still stratified at stations on the two northern lines, with salinities <35 only found at stations 16, 17, 21 and 22 and at the Wind Farm (29.14°N, 94.75°W). Further south, stations 1-10 and 13-15 all contained almost isohaline water with S>36.

The fresh water from the hurricane caused a major change in the surface salinity by the time of the first September cruise (22-27), resulting once again in a strong cross-shelf gradient (Fig. 4c).

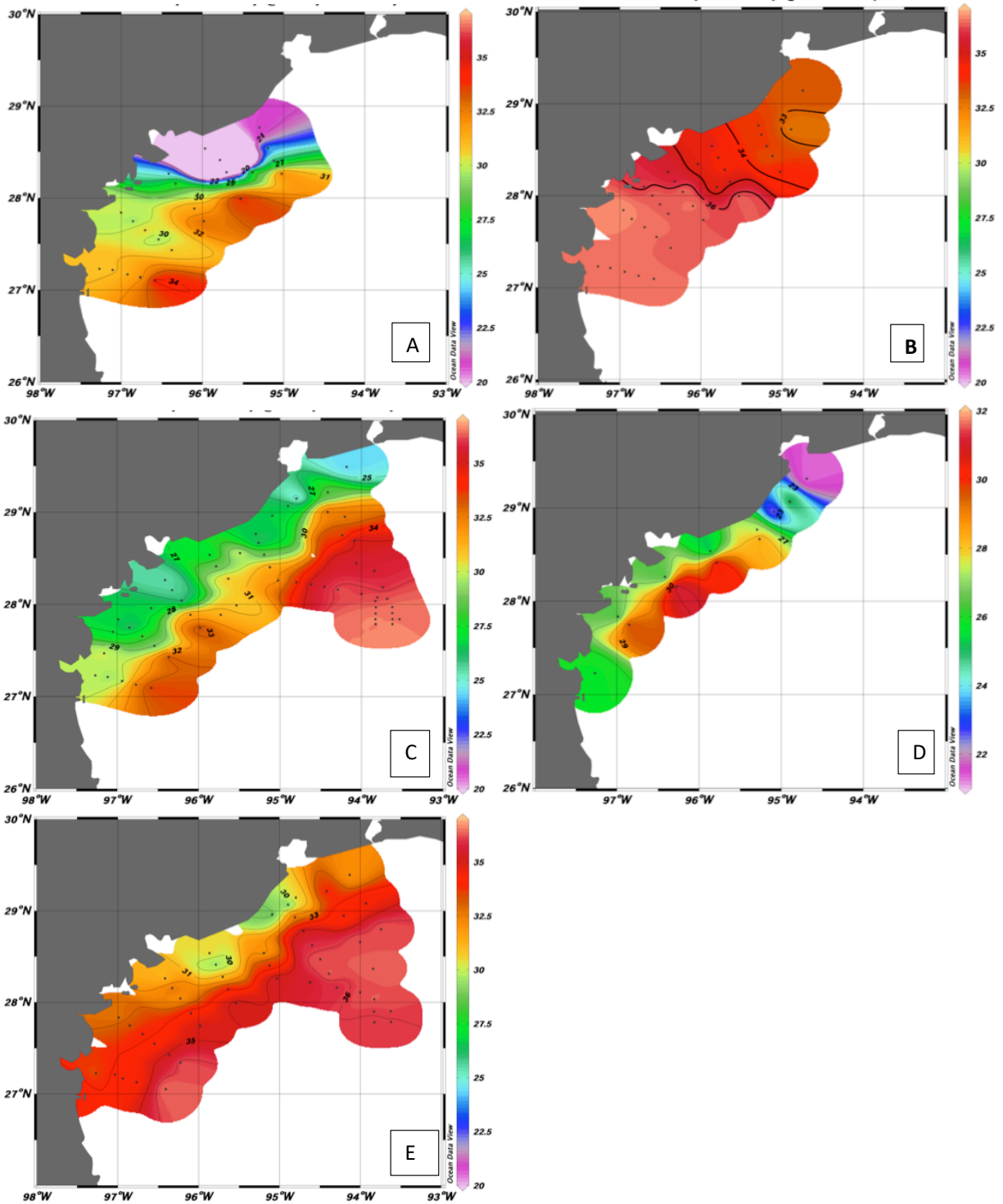


Fig. 4. Surface salinities during 2017 cruises in (a) June, (b) August, (c) 22-27 September, (d) 29 September – 1 October, and (e) November.

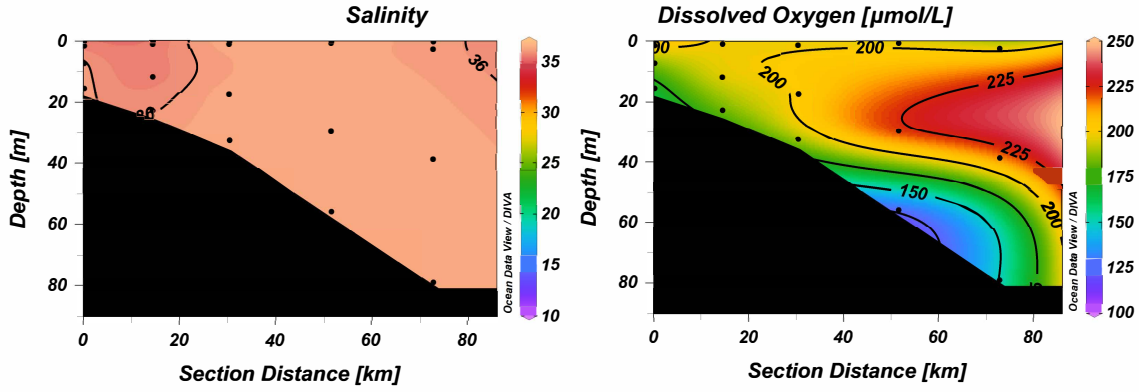
275

276

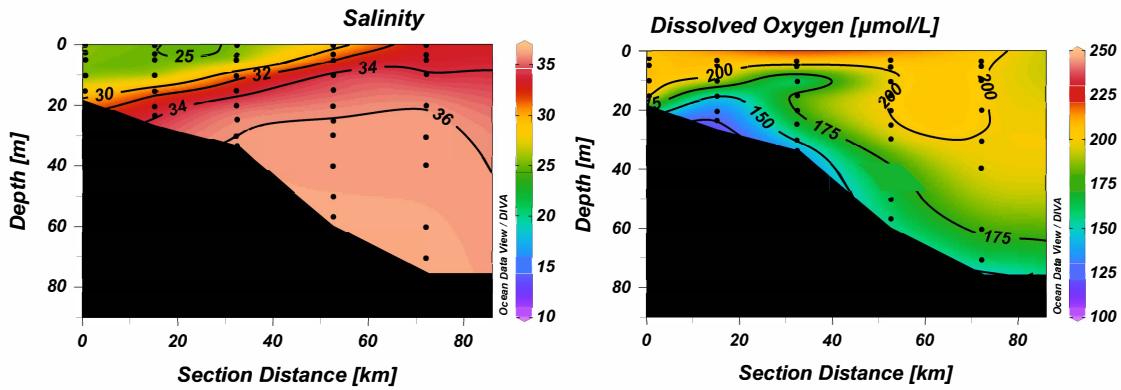
Surface salinities were <33 throughout the region, apart from two stations at the extreme south of the grid, and in the area more than 100 km offshore between Galveston Bay and the Flower Gardens Banks, where there was a strong salinity front. A similar situation was found a week later at the inshore stations (Fig. 4d), although the surface layer of low salinity water had thinned and was confined to the innermost stations on each line. Vertical sections in September showed very strong stratification of up to 10 in salinity within a 10-m depth interval along all lines (e.g., Fig. 5; this section across stations 11-15, adjacent to Matagorda Bay, is taken as representative for all five lines). The halocline was not flat, but deepened towards the coast, giving a wedge of low salinity water onshore, and the depth at which it intersected the bottom decreased from ~ 30 m in the north to less than 20 m in the south. Water with salinity > 36 was found at the bottom on all lines. By November (Figs 4e, 5), however, a more typical salinity field was found, with well-mixed water throughout the coastal zone and a general onshore-offshore gradient at all depths. This is normal for the region in the fall, when atmospheric frontal systems tend to move across the Texas shelf and break down the summer pycnocline (Cochrane and Kelly, 1986; Nowlin et al., 1998).

3.3 Oxygen concentrations

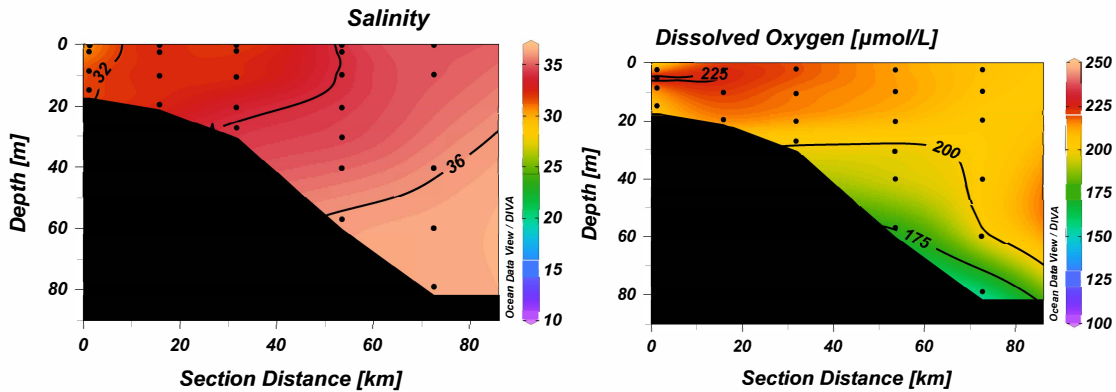
Oxygen concentrations in this region of the Gulf of Mexico are typically saturated above the pycnocline, as found during all four cruises. Concentrations varied between 210-220 $\mu\text{mol/L}$ in June (not shown), when the SST was about 25°C , and 190-215 $\mu\text{mol/L}$ during August and September, when it was nearer 30°C (Fig. 5). Oxygen saturation in seawater of salinity 35 is 206 $\mu\text{mol/L}$ at 25°C and 190 at 30°C . By November, with declining surface temperatures, the saturation concentration increased to between 210-230 $\mu\text{mol/L}$. Below the pycnocline, oxygen concentrations declined in the higher salinity water. This effect was most pronounced offshore in June and August, when subtropical underwater, with typical oxygen concentrations of 160-170 $\mu\text{mol/L}$, intruded onto the outer shelf (Fig. 5). Isolated patches with concentrations $<150 \mu\text{mol/L}$ were seen over the mid-shelf and across the eastern part of the grid at this time. By September, bottom concentrations of 150 $\mu\text{mol/L}$ or less were found over large parts of the inner and middle shelf and at the outermost stations of the grid. Vertical sections showed lowest oxygen concentrations at the base of the pycnocline where it intersected the seafloor (Fig. 5), but



A



B



C

Fig. 5. Salinity (psu) and oxygen ($\mu\text{mol/L}$) sections across line 3 (stations 11-15) for the August (a), first September (b) and November (c) cruises.

hypoxia (oxygen concentrations $<62 \mu\text{mol/L}$) was not observed at any station. There was little change in either the pattern of oxygen distribution or concentrations at the innermost stations

between the two cruises in September (not shown). By November, however, after the passage of a number of frontal systems with wind speeds up to 14 m/s, the oxygen concentrations showed little vertical structure and the system could be said to have returned to normal for that month.

3.4 Nutrients

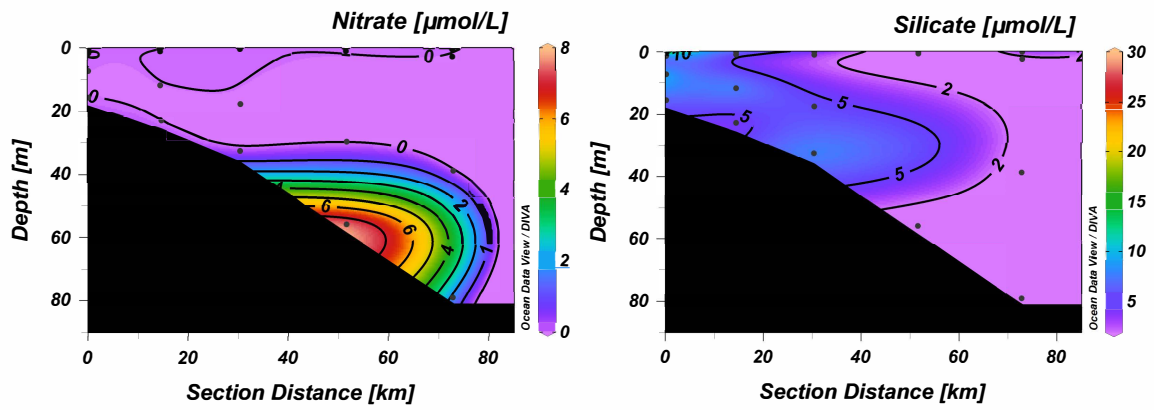
Nutrient concentrations in the coastal waters and bays along the Texas coast in summer are typically very low at the surface, increasing with depth even on the shallow shelf as nutrient regeneration takes place near the bottom. This is especially the case when hypoxic events occur (Nowlin et al., 1998; DiMarco and Zimmerle, 2017; Bianchi et al., 2010). Mean concentrations in the upper 30m of the water column for all nutrients at stations within the grid as well as at additional stations having water depths shallower than 50m are given in Table 2. Data from the second September cruise, which covered only the two inshore stations on each line, are not included in the table. These data showed similar patterns to the cruise a week earlier, although mean concentrations were higher because of the proximity of the coast and the many freshwater discharges from bays and rivers.

In higher salinity (>35) water and offshore, nutrient concentrations increase only slowly with depth and nitrate and silicate concentrations > 5 $\mu\text{mol/L}$ are generally found in midwater only below depths of about 50 and 100m respectively (Fig. 6, Supplemental Fig. S3). Only one nitrate sample (in September) containing more than 8 $\mu\text{mol/L}$ came from below 60m depth. Nitrite concentrations were almost all low, with mean concentrations in the upper 30m below 0.5 $\mu\text{mol/L}$ on all four cruises, although individual surface concentrations were considerably higher.

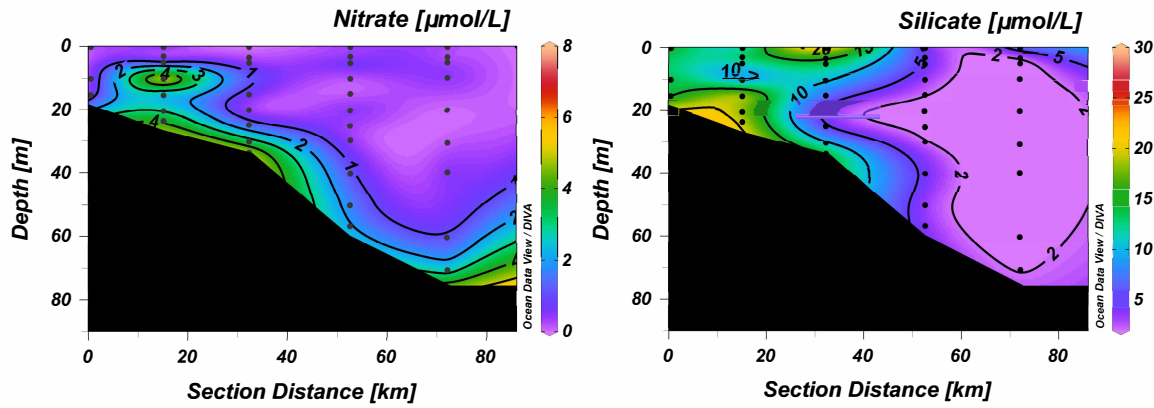
Ammonia concentrations were variable, particularly inshore, but generally provided a background concentration of about 2-4 $\mu\text{mol/L}$. As a result, DIN distribution resembled that for nitrate but with the added background contribution from ammonia (Fig. S4). Phosphate concentrations (not shown) were similarly lower at the surface than at depth, except in September, when surface runoff increased concentrations above 3 $\mu\text{mol/L}$ in the upper 10m of the water column and to a background concentration between 1.5 – 3 $\mu\text{mol/L}$ in the rest of the water column up to 50 km offshore (between stations 13 and 14). Phosphate is almost always non-limiting for phytoplankton in this region, so that residual phosphate concentrations can be

Table 2. Mean and range ($\mu\text{mol/L}$) and number of samples (N) for nitrate, nitrite, ammonia, phosphate and silicate in the upper 30m of the water column for all four cruises. DIN is calculated as the sum of the three nitrogen species. DIN:P and DIN:Si ratios use the values for all individual samples.

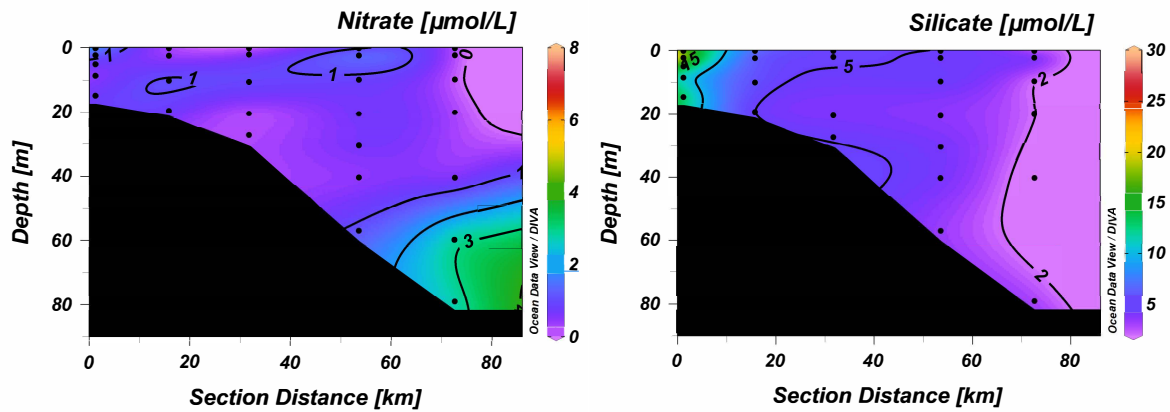
		June	August	September	November
Nitrate	Mean	0.71	0.10	0.57	0.52
	Range	0.00-10.60	0.00-1.98	0.00-7.41	0.00-1.98
	N	85	94	194	164
Nitrite	Mean	0.43	0.18	0.44	0.36
	Range	0.00-2.80	0.00-1.04	0.03-4.76	0.00-1.13
	N	86	98	196	172
Phosphate	Mean	1.07	0.65	1.30	1.00
	Range	0.21-2.85	0.00-3.55	0.00-5.63	0.00-3.24
	N	85	91	190	169
Silicate	Mean	6.00	5.04	7.00	7.76
	Range	1.18-26.89	0.00-20.09	0.00-40.23	0.94-25.71
	N	84	89	193	168
Ammonia	Mean	1.90	3.74	2.39	2.91
	Range	0.00-7.62	1.37-8.05	0.08-4.97	0.89-4.80
	N	84	87	192	162
DIN	Mean	3.01	3.70	3.37	3.72
	Range	0.01-14.47	0.14-8.56	1.02-12.35	1.05-7.03
	N	85	95	191	160
DIN:P		3.56	11.95	4.98	10.11
	Range	0.03-25.86	0.00-324	0.00-138	0.00-381
DIN:Si		0.63	2.59	1.17	0.78
	Range	0.00-3.20	0.00-53.29	0.00-25.21	0.10-4.78



A



B



C

Fig. 6. Nitrate and silicate ($\mu\text{mol/L}$) sections along line 3 (stations 11-15) during August (a), first September (b) and November (c) cruises.

found even though nitrate is depleted (Bianchi et al., 2010), although Sylvan et al. (2006, 2007) and Quigg et al. (2011) have suggested phosphate limitation can occur further east in the Mississippi plume. Silicate, however, showed an opposite trend to the general pattern of the other elements, with almost all samples $>15 \mu\text{mol/L}$ coming from the upper 25m of the water column, and concentrations decreased with depth to $<5 \mu\text{mol/L}$ below 100m (Figs 6, S3). Silicate also showed a cross-shelf gradient, particularly along the two southernmost lines (not shown).

This general distribution shown in Figs. 5 and 6 was seen during early summer along all the lines occupied during June and August. In June, high concentrations of both nitrate and silicate were seen at stations 21 and 22, immediately south of Galveston Bay, where bottom water oxygen concentrations were $< 90 \mu\text{mol/L}$; elsewhere midwater levels of both elements were low, with very low nitrate concentrations ($<0.5 \mu\text{mol/L}$) being found even at the bottom at some stations. While silicate concentrations were more variable, highest concentrations were typically again seen at the bottom, and midwater concentrations were generally $< 5 \mu\text{mol/L}$. The situation was similar in August (Fig. 6), when nitrate was very low throughout the region, and even bottom nitrate values were below detection at many stations.

In September, despite the extreme freshwater runoff, nitrate concentrations were still low except near the bottom at shallow stations, and there was little sign of any surface or mid-water increase in concentration (Fig. 6). A comparison of nitrate concentration with depth gave essentially the same distribution as during earlier cruises, although there were more samples above $2 \mu\text{mol/L}$ within the 10-30m depth range (Fig. S3). These were bottom samples at shallow stations with lower oxygen concentrations. The cross-shelf gradient in silicate concentrations was more pronounced on this cruise, and concentrations were $>10 \mu\text{mol/L}$ throughout the water column at all the inshore stations. However, by November, concentrations of both nutrients had decreased considerably, although the offshore silicate gradient was still present and concentrations $> 10 \mu\text{mol/L}$ were found inshore (Fig. 6). Phosphate concentrations higher than $2 \mu\text{mol/L}$ were seen only in September (Table 2), suggesting, along with the increased silicate, the presence of terrestrial runoff following the hurricane.

Oxygen/nitrate and oxygen/silicate covariance plots are shown in Supplemental Fig. S5. High nitrate values at oxygen concentrations greater than 200 $\mu\text{mol/L}$ in August and September (22-27) are from samples taken in low salinity surface water; where oxygen concentrations were below 150 $\mu\text{mol/L}$ the increase in nitrate concentration is caused either by regeneration over the shelf or by the intrusion of deeper Subtropical Underwater. During these two cruises, higher nitrate and silicate concentrations were associated generally with lower oxygen concentrations (Fig. S5), although some surface samples on both cruises showed relatively high values, associated with salinities < 35.

Quigg et al. (2011) state that DIN concentrations <1 $\mu\text{mol/L}$ and a DIN:P ratio <10 indicate nitrogen limitation, with P <0.2 $\mu\text{mol/L}$ and DIN:P >30 indicating P limitation and Si <2 $\mu\text{mol/L}$, DIN:Si >1 and Si:P <3 showing Si limitation. As shown in Table 2, DIN:P and DIN:Si ratios for individual samples in the upper 30m of the water column were low during all four cruises, with mean DIN:P being less than the 16:1 Redfield ratio throughout, while the mean DIN:Si ratio was >1 only in the August and September cruises. This suggests both nitrogen limitation throughout the period and possible silicate limitation of diatom growth during August and September despite the background levels of ammonia that contributed to the DIN concentration. While individual samples had higher ratios, these all occurred when either phosphate or silicate concentrations were measurable but very low in comparison with DIN concentrations (<0.1 $\mu\text{mol/L}$ for P and <0.5 $\mu\text{mol/L}$ for Si). The ratios of the mean concentrations of DIN across the region to the mean concentrations of P and Si (e.g., 3.01:1.07 for DIN:P in June), were 2.81 and 0.50, 5.69 and 0.73, 2.59 and 0.48, and 3.72 and 0.48 for the June, August, September and November cruises respectively, again suggesting nitrogen limitation.

3.5 Chlorophyll

Chlorophyll concentrations were examined using both in situ fluorescence data obtained during the cruises and satellite imagery from the MODIS sensor on the Aqua satellite (Fig. 7). The Texas coast and northwestern Gulf of Mexico were covered with clouds during the pre-Harvey and post-Harvey cruises, however a time-history of four high quality chlorophyll-*a* images on 18

August (pre-Harvey), 2 September (6 days post-Harvey), 11 September and 16 September 2017 revealed shelf events between the two cruises closest to Harvey's landfall.

Fluorescence data (not shown) from the CTD casts taken during all cruises were almost invariably $<1 \text{ mg m}^{-3}$, especially in the upper mixed layer, suggesting little productivity immediately before or during the cruises. During the 22-27 September cruise only 4 of 37

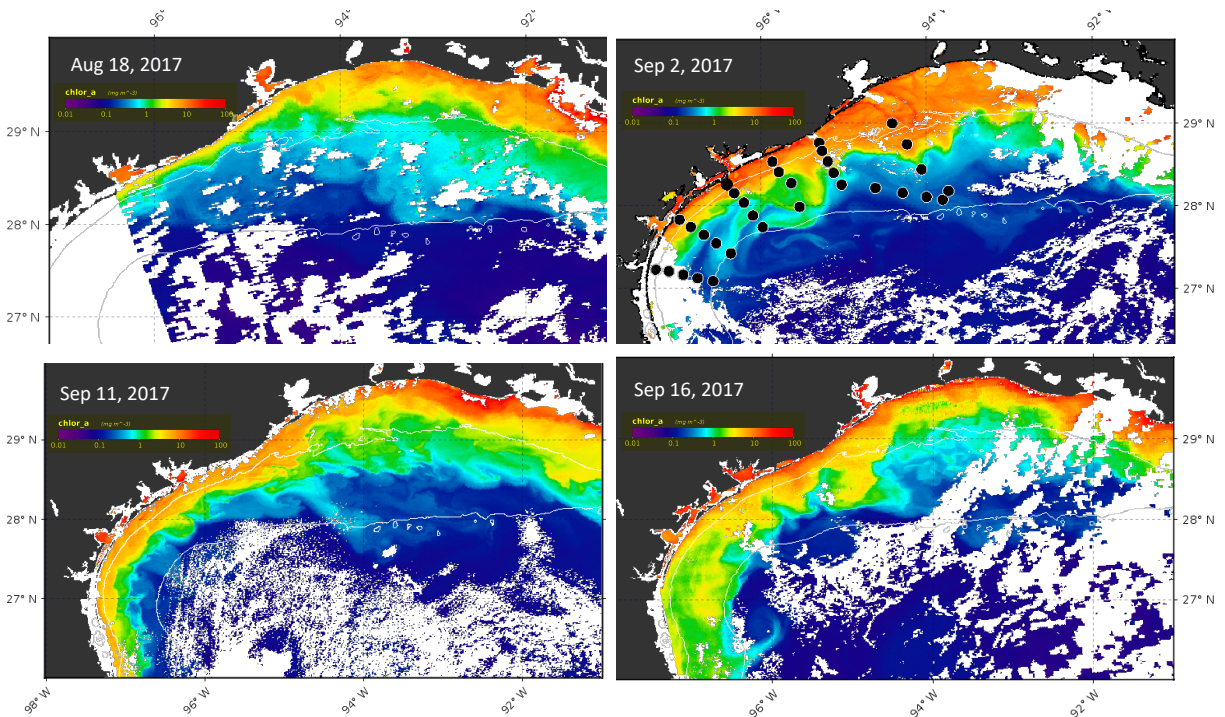


Fig. 7. Aqua-1 MODIS imagery depicting chlorophyll *a* estimates for 18 August, 2 September, 11 September and 16 September, 2017. White areas along the Louisiana shelf and offshore are clouds. Thin white lines denote 20m and 100m isobaths. Station positions are indicated by the black dots on the 2 September image.

stations had concentrations $>1.0 \text{ mg m}^{-3}$, while at 29 stations they were 0.5 mg m^{-3} or less. The highest surface concentration (1.7 mg m^{-3}) was found inshore just south of Galveston Bay. Midwater maxima only exceeded 2 mg m^{-3} below 40m depth at offshore stations 27 and 28. This is similar to summer conditions reported by Nowlin et al. (1998) and to previous data we have collected during summer cruises in the northern Gulf of Mexico. Three days later, however, when the inshore stations were reoccupied, mean fluorescence values showed $1\text{-}2 \text{ mg m}^{-3}$ at all inshore stations, with concentrations up to 4.8 mg m^{-3} immediately offshore of Galveston in the plume.

Satellite data, in contrast, showed considerably higher pigment values (Fig. 7). During mid-August, the highest concentrations and the maximum offshore extent of potential blooms were found off central Louisiana, within the 20m isobath. The zone of pigmented water narrowed significantly from Sabine Lake (93.83°W) to Port Aransas Bay (97°W). This distribution likely resulted from the pre-storm advection of nutrients from the Atchafalaya and Mississippi Rivers coupled with generally low summer flows from Texas rivers. By 2 September, the highest concentrations were detectable along the Texas coast from Sabine Lake to Corpus Christi Bay. The widest zone of pigmented water extended well beyond the 20 m isobath east, southeast, and south of Galveston Bay. Maximum satellite-derived coastal chlorophyll-*a* values near Galveston Bay were 16 mg m⁻³, decreasing offshore to 10 mg m⁻³ at the 20 m isobath, and below 1 mg m⁻³ on the 100 m isobath (Fig. 8). During September, the zone of pigmented water on the shelf near Galveston initially retreated shoreward, but moved offshore and southward later, with several lobes reaching the 100 m isobath, although concentrations were only about one tenth of those seen immediately after the storm.

4 Discussion

Previous studies of the impacts of hurricanes on the coastal zone suggest that the extreme rainfall associated with such storms often leads to flushing of nutrients into the coastal bays and the offshore coastal zone, as found in Biscayne Bay, Florida, following Hurricane Katrina in 2005 (Zhang et al., 2009), in the Neuse River/Pamlico Sound system in North Carolina (Paerl et al., 2001, 2018; Peierls et al., 2003), in Chesapeake Bay (Roman et al., 2005), and in the Caribbean in 1998 following Hurricane Georges (Gilbes et al., 2001). In all these cases, short-lived phytoplankton blooms (2-3 weeks) resulted. It is also possible for offshore waters containing low oxygen concentrations and raised nutrient concentrations to be injected onto the shelf from offshore through upwelling. Chen et al. (2003), for example, while agreeing with Shiah et al. (2000) that terrestrial runoff was a factor in increased local coastal productivity following such storms in the East China Sea, suggested that the upwelling of subsurface Kuroshio water, thought to result from “a larger buoyancy effect caused by the rains as well as the shoreward movement of the Kuroshio caused by the typhoons,” was equally important, and that the “cross-shelf

upwelling of nutrient-rich Kuroshio water after the passage of typhoon Herb in a normally downwelling region” could even induce local hypoxia.

A third potential impact is local acidification resulting from the excessive rainfall in the coastal region, as reported by Manzello et al. (2013) and Gray et al. (2012). Hicks et al. (2022) showed that this occurred in Galveston Bay following Harvey, with the acidification lasting for three weeks and causing undersaturation of calcium carbonate that may have affected the recovery of local oyster reefs.

Oxygen and nutrient variability

Our data show very little sign of increased nutrient concentrations offshore, other than excess phosphate seen during the first September cruise. Since Texas bays are oligotrophic during the summer, the influx of freshwater resulted in higher concentrations of nutrients, particularly nitrate and silicate, as well as blooms of phytoplankton and cyanobacteria within the bays (Liu et al., 2019; Steichen et al., 2020). DIN concentrations, in particular, were greatly reduced two weeks after the hurricane had passed through the region and were back to normal conditions by November (Steichen et al., 2020, Fig. 8; J. Fitzsimmons, pers. comm.), with concentrations above 5 $\mu\text{mol/L}$ only found in the uppermost parts of the system after about 15 September. Silicate concentrations similarly dropped quickly within the first two weeks, although they remained above 40 $\mu\text{mol/L}$ throughout Galveston Bay during the sampling period.

Following hurricane Harvey, low-oxygen water containing $<160 \mu\text{mol/L}$ and nitrate concentrations of $> 2 \mu\text{mol/L}$ penetrated further onto the shelf during September than during either August or November (Figs. 5, S3). The high salinity of this water mass (>36 , Fig. 5) suggests that it was Subtropical Underwater, which is found above 250 m in the northern Gulf with typical core salinity of about 36.4 -36.5 near 100m depth in this region, and oxygen and nitrate concentrations of about 110-150 $\mu\text{mol/L}$ and 6-15 $\mu\text{mol/L}$ respectively (Nowlin et al., 1998). However, given the strong pycnocline shown by the salinity section (Fig. 5), there was little opportunity for these additional nutrients to reach the surface layer and affect phytoplankton production, and there is no evidence that such upwelling has resulted in hypoxia in the past in this region.

494
495 Further south, the Matagorda-San Antonio-Aransas-Corpus Christi Bay system also showed
496 rapid short-term nutrient increases, followed in this case by hypoxia (Montagna et al., 2017;
497 Walker et al., 2021), but nutrient concentrations here were back to pre-storm concentrations by
498 early October (Walker et al., 2021). The levels in Guadeloupe Bay, an offshoot of San Antonio
499 Bay, were followed at fortnightly intervals from mid-August to mid-October and showed a rapid
500 increase in nitrate but slower increases in phosphate and silicate. This is not unexpected, given
501 that nitrate does not bind readily to sediment particles or organo-iron complexes like phosphate
502 and silicate (Lewin, 1961; Suess, 1981). Thus, it appears that the increases in nutrient
503 concentrations affected mainly the coastal bays and estuaries rather than the offshore coastal
504 zone. This backs up conclusions of Sahl et al. (1993) following a cruise along the Louisiana-
505 Texas shelf in March 1989 when river discharges were at their highest levels during that year.
506 They found that nutrients derived from bay systems dissipated within about 20km of the bay
507 mouths, and that higher nutrient concentrations below 80 m depth resulted from upwelling along
508 the shelf edge, in agreement with the work of Chen et al. (2003) and Walker et al. (2005).

509
510 Although nutrient fluxes were undoubtedly greatly increased immediately following the
511 hurricane, nutrient concentrations in Texas rivers are only sampled infrequently, and data do not
512 exist to allow us to calculate the overall fluxes during this period. However, the available data
513 suggest that absolute concentrations did not change very much following the hurricane in most
514 instances (Table 3). Coupled with the rapid decrease in river flow by about 7 September (Fig.
515 S1), this suggests that excess nutrients in the bays and the coastal ocean were likely either taken
516 up by phytoplankton (within the bays) or diluted (offshore) by the time of our survey in late
517 September. Du et al. (2019) point out that while the salinity at the mouth of Galveston Bay was
518 back to normal about two weeks after the storm, it took almost two months to recover at stations
519 further inside the bay and the same time period at offshore buoys. Similar effects are likely at
520 other bay sites along the Texas coast.

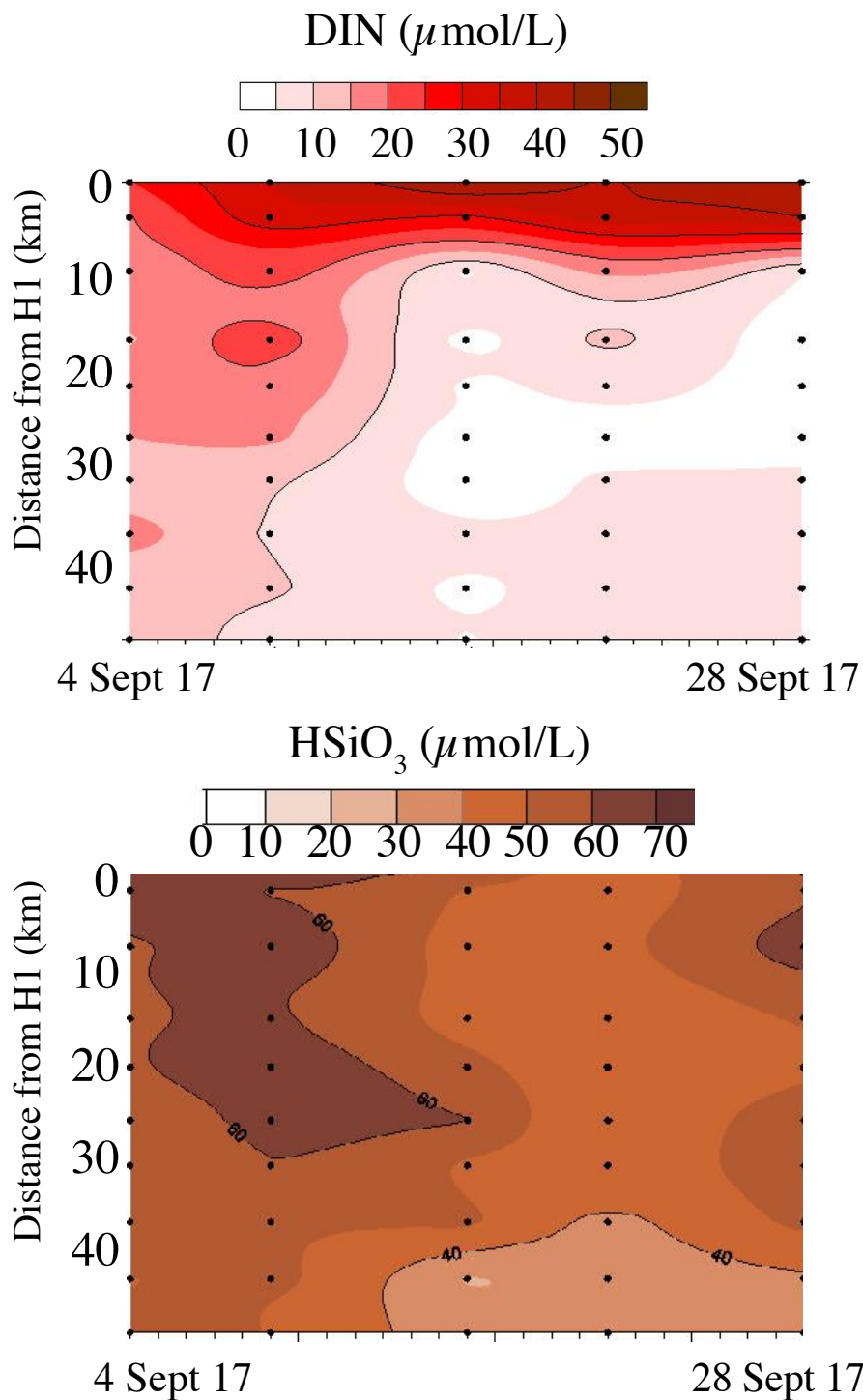


Fig. 8. Surface nitrate plus nitrite (a) and silicate (b) concentrations ($\mu\text{mol/L}$) measured along a transect through Galveston Bay along the Houston Ship Channel. Sampling dates were 4 September, 9 September, 16 September, 21 September, and 28 September 2017. Station H1 (0 km) was the innermost station in the bay, H10 was just outside the breakwater in the Gulf (see Steichen et al., 2020 for details).

Table 3. Nutrient concentrations in Texas rivers around the time of the hurricane ($\mu\text{mol/L}$). Data taken from USGS and the Texas Commission on Environmental Quality (TCEQ) Clean Rivers Program for individual river basins.

a. Trinity River (Baytown; USGS site 08067525)

Date	Nitrate	Phosphate	Silicate
7.06.17	10.15	2.03	74.2
7.19.17	11.28	2.52	90.0
8.15.17	11.43	3.16	155.5
9.05.19	10.64	1.74	96.0
11.08.17	5.43	1.58	143.5

b. Trinity River (Liberty, USGS site 08067000)

8.16.17	<2.86	2.38	137.5
8.31.16	8.71	1.32	97.8
9.05.16	15.85	2.26	127.0

c. Brazos River (US 290; TCEQ site 11850)

7.26.17	41.40	<1.29
8.22.17	7.86	<1.29
9.27.17	12.86	2.26
10.25.17	37.86	2.90

d. Colorado River (La Grange; TCEQ site 12292)

6.06.17	2.86	92.58
8.08.17	2.86	118.06
10.02.17	2.14	86.45

e. San Antonio River (Goliad; TCEQ site 12791)

7.19.17	<3.57
9.06.17	<3.57
11.01.17	<3.57

Salinity variability in the coastal zone

Salinity changes were recorded at offshore moorings during and following the storms. During the passage of the hurricane, the TABS moorings showed rapid decreases in salinity with a slow increase thereafter (data not shown). Buoy X (offshore) showed the least variability, with salinities remaining near 36.4 until 4 September 2017, dropping briefly to 35.3, but recovering to above 36 again by 6 September. Buoy D, inshore near Corpus Christi, also recorded salinities of about 36.6 until 23 August, dropping to 34.7 on 26 August, but were >36 a day later. Salinities dropped again on 29 August, remaining in the range 32-34 until 6 September, after which they dropped again to below 30, where they remained until 24 October 2017, with a minimum salinity

of 20.51 on 13 September. Further up the coast buoys B and F both experienced decreased salinities (buoy W did not record salinities during the passage of the hurricane). Before the hurricane, salinities in this region were in the range 32.5-34.5, with the higher salinities offshore. Following the passage of the storm, buoy F recorded a minimum salinity of 15.25 on 1 September and salinities <20 until 6 September. A salinity of 30 was only recorded again here on 8 September. The inshore buoy B recorded minimum salinities in the range 19-21 on 30 August. These remained <23 until 9 September, and below 30 for the remainder of the month, after which they increased again to around 32. The fact that the minimum salinity was recorded at the offshore mooring is presumably related to the strength of the plume emanating from Galveston Bay with enough momentum to overcome the Coriolis force that would tend to push it to the southwest close to the coast (Du et al., 2019).

These data suggest a slow southward movement of low salinity water along the coast (see Figs. 4c, d) after the hurricane as the coastal current was re-established. The easterly winds during almost the whole of September assisted this downcoast movement, as described by Cochrane and Kelly (1986). Mixing during the infrequent northerly wind bursts caused salinities to increase again, although even in November salinities below 30 were still seen between Galveston Bay and Matagorda-Corpus Christi Bays (Fig. 4e).

Chlorophyll variability

Assuming that chlorophyll-*a* can be used as a proxy for phytoplankton productivity, along the Texas shelf and slope, we can use the MODIS satellite data to show how the phytoplankton biomass varied following the hurricane. The prevailing currents during the latter half of September (Fig. 3), would have moved the pigment concentrations further south and offshore, where they decreased. Since our first post-storm cruise occurred between 22-27 September, we would have missed the maximum extent of any offshore nutrient maximum and its associated bloom. Given the potential discrepancy between satellite-derived and in situ values from CDOM interference in the satellite estimates, however, we believe the higher concentrations in early September shown in Fig. 7 result largely from the hurricane stirring up bottom sediments in the shallow coastal zone, and there was no evidence for upwelled nutrients resulting in blooms at the shelf edge, as reported off Louisiana following Hurricane Ivan in 2004 (Walker et al., 2005) or in

the East China Sea by Chen et al. (2003). The accumulation of highly pigmented water between Galveston Bay and Calcasieu Lake (93.45°W) in the 2 September image likely resulted from convergence of the downcoast Louisiana river waters (Quigg et al., 2011) with upcoast hurricane-related discharges from Texas, as surface currents at TABS buoy B were offshore and decreased from ~75 cm/s to 20 cm/s during the period from 30 August to 3 September (Fig. 3).

Why was there no hypoxia following Harvey?

Although September is normally the month when the passage of storm front causes seasonal hypoxia (oxygen concentrations <62 $\mu\text{mol/L}$) in the northern Gulf of Mexico to end, the strong stratification resulting from the freshwater input might have been expected to reduce oxygen concentrations below the pycnocline. Rabalais et al. (1999) state that hypoxia can in fact occur in almost any month if conditions, particularly stratification, are right. Hypoxia in the northern Gulf of Mexico has three requirements: a high supply of nutrients, especially nitrogen, from rivers or other terrestrial runoff, stable stratification with a mid-water pycnocline, and relatively low wind conditions (Bianchi et al., 2010; Rabalais et al., 2007; Wiseman et al., 1997). While the most intense hypoxia occurs over the Louisiana shelf (Rabalais et al., 1999), dissolved oxygen levels below 30 $\mu\text{mol/L}$ have been detected during NOAA SEAMAP cruises as far west as 96°W, with occasional samples between 30-60 $\mu\text{mol/L}$ identified near Corpus Christi (see <https://www.ncei.noaa.gov/maps/gulf-data-atlas/atlas.htm>, accessed 16 July 2020), as well as following local flood events (DiMarco et al., 2012; Kealoha et al., 2020), and bacteria from terrestrial sources have been found in sponges at the Flower Gardens Banks National Marine Sanctuary near 28°N, 29.5°W (Shore et al., 2021).

While Texas hypoxia is typically linked to southwestward advection from the Mississippi and Atchafalaya Rivers, high flow rates from local rivers have also been implicated (Harper et al., 1981; Pokryfki and Randall, 1987; DiMarco et al., 2012). During the passage of Hurricane Harvey, the torrential rainfall led to runoff that created a stable pycnocline, and calm conditions after the storm meant that phytoplankton growth was possible. On the Louisiana shelf, stratification is re-established within a few days of the passage of storm fronts or hurricanes and bottom water oxygen depletion can begin rapidly once the storm has passed (e.g., Bianchi et al., 2010; Jarvis et al., 2021). However, despite the strong stratification after Harvey, we found no

obvious signs of hypoxia over the Texas shelf, nor any increased nutrient concentrations, other than phosphate, in coastal water. Plotting the difference in salinity between surface and bottom samples, a measure of water column stability (DiMarco et al., 2012), against bottom oxygen concentrations during the September cruise gave only a low correlation, with $R^2 = 0.15$ ($n = 38$), as opposed to the 0.79 ($n = 14$) reported in 2007 by DiMarco et al. (2012). This suggests that stratification by itself was not responsible for the observed bottom oxygen concentrations over the shelf following Harvey.

The lack of hypoxia following Hurricane Harvey can therefore perhaps be explained by four factors. First, only a limited flux of nutrients made it out of the bays and into the coastal zone, where it was likely taken up rapidly by phytoplankton in the oligotrophic coastal waters, as seen elsewhere. Additionally, southward and offshore advection of low salinity runoff increased the rate of dilution through mixing with pre-existing low-nutrient surface shelf water. The largest bay systems have relatively narrow entrances, which reduce the rate at which the fresh water can escape – the main entrance to Galveston Bay, which includes the deep, dredged Houston Ship Channel, is only 2.3 km wide and the turnover time for water is 15-60 days under normal conditions, with shorter periods coinciding with flood conditions (Solis and Powell, 1999; Rayson et al., 2016). Thyng et al. (2020) have estimated that the flushing of Galveston Bay during Hurricane Harvey took only 2-3 days following the initial heavy rainfall. For the Corpus Christi Bay/Aransas Bay system the turnover time under normal conditions is estimated to be more than 300 days (Solis and Powell, 1999), similar to Pamlico Sound (Paerl et al., 2001).

Second, the sheer volume of water rapidly removed available soluble nutrients within the first few hours so that runoff later during the storm was essentially pure rainwater. It is known that large percentages of available nutrients are removed in stormwater runoff in the first minutes or hours following a downpour and concentrations then drop (e.g., Cordery, 1977; Horner et al., 1994; Fellman et al., 2008). Similar effects have been reported for trace metals in the floodplain of the Pearl River in Mississippi (Shim et al., 2017), where maximum downstream concentrations were not found following peak flows. These authors suggested that the rapid flushing overwhelmed the rate at which soluble metal-organic complexes could be regenerated. As the hurricane occurred in late summer, any nutrients applied to cropland along the Texas

coastline in spring would largely have been taken up by the vegetation and so be unavailable for washout. While Corpus Christi (population ~325,000) and Houston (~4 million) are large population centers with multiple sewage treatment plants that flooded following the hurricane, both are sited upstream of large bay systems that would have attenuated the speed at which stormwater runoff dissipated. The rate of change of nutrient concentrations in Galveston Bay (Fig. 8) shows that uptake within the bay system was likely considerably more important than flushing, even with the apparently short flushing time calculated by Thyng et al (2020).

While nutrient flushing was reduced following the hurricane, the same is unlikely to be true for sediment. As shown in Fig. S2, and as discussed by D'Sa et al. (2018), Du et al. (2019), and Steichen et al. (2020), large sediment plumes occurred off the mouths of major bays and rivers. The heavy sediment loads would have both increased the turbidity of the water column and thereby reduced light intensity in the euphotic zone, and led to reduced phosphate concentrations as phosphate is known to bind to sediment particles (e.g., Suess, 1981). Both factors would have contributed to reduced phytoplankton production, a major factor in hypoxia formation (Bianchi et al., 2010). While phosphate concentrations in the coastal zone were highest during the first September cruise, suggesting at least some terrestrial runoff immediately following the hurricane and possibly desorption from suspended sediment, the low nitrate concentrations seen during this cruise and the low chlorophyll fluorescence suggests only a short-term phytoplankton bloom at most, again similar to previous observations (e.g., Roman et al., 2005).

The final potential control is sediment composition along the Texas shelf. Most sediments in this region are coarse, sandy, and contain little organic matter (Hedges and Parker, 1974). This is in contrast to the Louisiana shelf, where muddy, organic sediments are quite common and act as a reservoir of material that can continue to reduce oxygen concentrations once stratification is established (Bianchi et al., 2010; Corbett et al., 2006; Eldridge and Morse, 2008; Turner et al., 2008). This is especially true within coastal embayments, such as Terrebonne Bay, LA, where the organic carbon content can exceed 5% thanks to organic matter input from the surrounding marshes and swamps (Hedges and Parker, 1974; Bianchi et al., 2009, 2010). Even near the Mississippi and Atchafalaya Rivers, however, typical organic carbon sediment content on the shelf is generally <2% (Gordon and Goni, 2004; Gearing et al, 1977), while further west off the

Texas coast it is typically $< 1\%$ (Hedges and Parker, 1974, Bianchi et al., 1997). This suggests that organic matter along the Texas shelf is refractory, and less likely to add to any oxygen demand, and that hypoxia on the Texas shelf is generally driven by water column respiration as discussed by Hetland and DiMarco (2008). In this region stratification alone is not sufficient to bring about hypoxic conditions in the absence of high nutrient concentrations and phytoplankton blooms.

5 Conclusions

Although Hurricane Harvey led to pronounced flooding and exceptional freshwater runoff along the Texas coast, it did not lead to lasting high nutrient concentrations offshore, largely because of dilution by the rainfall, the likely rapid uptake by phytoplankton of nutrients within the bays, and mixing with oligotrophic coastal water. While the most pronounced changes in nutrient concentrations were seen in the coastal bays, changes from background levels were short-lived, and conditions were essentially back to normal by November, some eight weeks after the hurricane, following northerly wind bursts that caused mixing within the water column. There was also no evidence of low oxygen water upwelled by the hurricane reaching the inner shelf from offshore, as suggested following hurricanes elsewhere. While an apparent transient bloom of phytoplankton was observed in satellite imagery offshore following the hurricane, its short existence and the potential for contamination of satellite estimates by CDOM suggests that hypoxia could not develop despite the stratification because nutrient concentrations were too low to support continued phytoplankton productivity. Similarly, the lack of an organic matter reservoir in the shelf sediments means there is no additional oxygen demand in Texas bottom waters, and hypoxia here depends on water column decomposition.

6 Acknowledgements

We are grateful to the Captains and crews of the R.V. *Manta* and R.V. *Point Sur* for their excellent service during the cruises, and to the enthusiasm of the students and technicians who helped with data collection. The TABS system is funded by the Texas General Land Office and operated by the TAMU Geochemical and Environmental Research Group. Cruises were funded by the Texas Governor's Fund through the Texas OneGulf Center of Excellence and an NSF RAPID award (OCE-1760381) to Drs. Knap, Chapman and DiMarco. A.H. K. would also like to

acknowledge financial support from the G. Unger Vetlesen Foundation. We thank Ysabel Wang and Jamie Steichen for help with the figures, and Alaric Haag for assistance with SeaDAS image processing. Walker and Haag thank the Gulf of Mexico Coastal Ocean Observing System (GCOOS) for funding LSU Earth Scan Laboratory activities. Bathymetry shown in satellite imagery was provided by GEBCO Compilation Group (2020) GEBCO 2020 Grid (doi:10.5285/a29c5465-b138-234d-e053-6c86abc040b9). Funding sources had no involvement in study design, data collection and interpretation, or manuscript preparation.

Data have been submitted to the Biological and Chemical Oceanography Data Management Office (BCO-DMO). The titles and DOIs are: Processed CTD profile data from all electronic sensors mounted on rosette from R/V Pt. Sur PS 18-09 Legs 01 and 03, Hurricane Harvey RAPID Response cruise (western Gulf of Mexico) September-October 2017 (DOI:10.26008/1912/bco-dmo.809428.1); Hydrographic, nutrient and oxygen data from CTD bottles and beam transmission and fluorescence data from CTD profiles during R/V Point Sur PS1809 (HRR legs 1, 2, 3) at the Gulf Mexico, Louisiana and Texas coast, Sept-Oct 2017 (doi:10.1575/1912/bco-dmo.784290.1).

7 Credit author statement

The project was conceptualized by SFD and AHK; PC and SFD conducted investigations on all cruises and collected and analyzed the initial data; AQ provided data from Galveston Bay; NDW provided satellite imagery. PC wrote the initial draft; all authors provided comments and edits. The authors declare that they have no conflict of interest.

References

- Ahn, J.H., Grant, S.B., Surbeck, C.Q., DiGiacomo, P.M., Nexlin, N., Jiang, S.: Coastal Water Quality Impact of Stormwater Runoff from an Urban Watershed in Southern California. *Environ. Sci. Technol.*, 39, 5940-5963, doi:10.1021/es0501464, 2005
- Balaguru, K., Foltz, G.R., Leung, L.R.: Increasing magnitude of hurricane rapid intensification in the central and eastern tropical Atlantic. *Geophys. Res. Lett.*, 45, 4238–4247, doi: 10.1029/2018GL077597, 2018
- Bianchi, T.S., DiMarco, S.F., Smith, R.W., Schreiner, K.M.: A gradient of dissolved organic carbon and lignin from Terrebonne-Timbalier Bay estuary to the Louisiana shelf (USA). *Mar. Chem.*, 117, 32-41, doi: 10.1016/j.marchem.2009.07.010, 2009.
- Bianchi, T.S., DiMarco, S.F., Cowan, J.H., Hetland, R.D., Chapman, P., Day, J.W., Allison, M.A.: The Science of Hypoxia in the Northern Gulf of Mexico: A Review. *Sci. Total Environ.*, 408, 1471-1484; doi: 10.1016/j.scitotenv.2009.11.047, 2010.
- Bianchi, T.S., Lambert, C.D., Santschi, P.H., Guo, L.: Sources and transport of land-derived particulate and dissolved organic matter in the Gulf of Mexico (Texas slope/shelf): The use of lignin-phenols and loliolides as biomarkers. *Org. Geochem.*, 27, 65-78, doi: 10.1016/S0146-6380(97)00040-5, 1997.
- Blake, E.S., Zelinsky, D.A.: *Hurricane Harvey*. NOAA National Hurricane Center Tropical Cyclone Report AL092017, 2018.
- Chen, C-T. A., Liu, C-T., Chuang, W.S., Yang, Y.J., Shiah, F-K., Tang, T.Y., Chung, S.W.: Enhanced buoyancy and hence upwelling of subsurface Kuroshio waters after a typhoon in the southern East China Sea. *J. Mar. Sys.*, 42, 65-79, doi :10.1016/S0924-7963(03)00065-4, 2003.
- Cochrane, J.D., Kelly F.J.: Low-frequency circulation on the Texas-Louisiana continental shelf. *J. Geophys. Res.* 91, 10645-10659, doi: 10.1029/JC091iC09p10645, 1986.
- Corbett, D.R., McKee, R.A., Allison, M.A.: Nature of decadal-scale sediment accumulation in the Mississippi River deltaic region. *Cont. Shelf Res.*, 26, 2125-2140, doi: 10.1016/j.csr.2006.07.012, 2006.
- Cordery, I.: Quality characteristics of urban storm water in Sydney, Australia. *Water Resources Res.*, 13, 197-202, doi: 10.1029/WR013i001p00197, 1977.

775 De Carlo, E., Hoover, D.J., Young, C.W., Hoover, R.S., Mackenzie, F.T.: Impact of storm runoff
 776 from tropical watersheds on coastal water quality and productivity. *Appl. Geochem.*, 22,
 777 1777-1797. doi: 10.1016/j.apgeochem.2007.03.034, 2007.

778 DiMarco, S.F., Strauss, J., May, N., Mullins-Perry, R.L., Grossman, E. Shormann, D.: Texas
 779 coastal hypoxia linked to Brazos River discharge as revealed by oxygen isotopes. *Aq.*
 780 *Geochem.*, 18, 159-181, doi:10.1007/s10498-011-9156-x, 2012.

781 DiMarco, S.F., Zimmerle, H.M. 2017. *MCH Atlas: Oceanographic Observations of the*
 782 *Mechanisms Controlling Hypoxia Project*. Texas A&M University, Texas Sea Grant
 783 Publication TAMU-SG-17-601, 300 pp. (available online at <http://mchatlas.tamu.edu>).

784 D'Sa, E., Joshi, I., Liu, B.: Galveston Bay and coastal ocean optical-geochemical response to
 785 Hurricane Harvey from VIIRS ocean color. *Geophys. Res. Lett.*, 45, 10,579-10,589
 786 doi:10.1029/2018GL079954 2018.

787 Du, J., Park, K., Dellapenna, T.M., Clay, J.C.: Dramatic hydrodynamic and sedimentary
 788 responses in Galveston Bay and adjacent inner shelf to Hurricane Harvey. *Sci. Total.*
 789 *Environ.*, 653, 554-564, doi: 10.1016/j.scitotenv.2018.10.403, 2019.

790 Eldridge, P.M., Morse, J.W.: Origins and temporal scales of hypoxia on the Louisiana shelf:
 791 importance of benthic and sub-pycnocline water column metabolism. *Mar. Chem.*, 108, 159-
 792 171, doi: 10.1016/j.marchem.2007.11.009, 2008.

793 Emanuel, K.: Assessing the present and future probability of Hurricane Harvey's
 794 rainfall. *Proc. Natl. Acad. Sci. U.S.A.*, 114, 12681–12684, doi:10.1073/
 795 pnas.1716222114, 2017.

796 Fellman, J.B., Hood, E., Edwards, R.T., D'Amore, D.V.: Return of salmon-derived nutrients
 797 from the riparian zone to the stream during a storm in southeastern Alaska. *Ecosystems*, 11,
 798 537-544, doi: 10.1007/s10021-008-9139-y, 2008.

799 Fritz, A., Samenow, J. 2017. Harvey Unloaded 33 Trillion Gallons of Water in the U.S. The
 800 Washington Post, September 2, 2017. [https://www.washingtonpost.com/news/capital-weather-](https://www.washingtonpost.com/news/capital-weather-gang/wp/2017/08/30/harvey-has-unloaded-24-5-trillion-gallons-of-water-on-texas-and-louisiana/)
 801 [gang/wp/2017/08/30/harvey-has-unloaded-24-5-trillion-gallons-of-water-on-texas-and-](https://www.washingtonpost.com/news/capital-weather-gang/wp/2017/08/30/harvey-has-unloaded-24-5-trillion-gallons-of-water-on-texas-and-louisiana/)
 802 [louisiana/](https://www.washingtonpost.com/news/capital-weather-gang/wp/2017/08/30/harvey-has-unloaded-24-5-trillion-gallons-of-water-on-texas-and-louisiana/).

803 Gearing, P., Plucker, F.T., Parker, P.L.: Organic carbon stable isotope ratios of continental
 804 margin sediments. *Mar. Chem.*, 5, 251-266, doi: 10.1016/0304-4203(77)90020-2, 1977.

805 Gilbes, F., Armstrong, R.A., Webb, R.M.T., Muller-Karger, F.E.: SeaWiFS helps assess
 806 hurricane impact on phytoplankton in Caribbean Sea. *Eos, Trans. Amer. Geophys. Union*, 82,
 807 529, 533, doi: 10.1029/01EO00314, 2001.

808 Gordon, E.S., Goni, M.A.: Controls on the distribution and accumulation of terrigenous organic
 809 matter in sediments from the Mississippi and Atchafalaya river margin. *Mar. Chem.*, 92, 331-
 810 352, doi: 10.1016/j.marchem.2004.06.035, 2004.

811 Gray, S.E.C., DeGrandpre, M.D., Langsdon, C., Corredor, J.E. Short-term and seasonal pH,
 812 pCO₂ and saturation state variability in a coral reef ecosystem. *Glob. Biogeochem. Cycles*
 813 26, GB3012, 2012.

814 Harper, D.E. Jr., Salzer R.R., Case R.J.: The occurrence of hypoxic bottom water off the upper
 815 Texas coast and its effect on the benthic biota. *Contr. Mar. Sci.*, 24, 53-79, 1981.

816 Hedges, J.I. , Parker, P.L.: Land-derived organic matter in surface sediments from the Gulf of
 817 Mexico. *Geochim. Cosmochim. Acta*, 40, 1019-1029, doi: 10.1016/0016-7037(76)90044-2,
 818 1974.

819 Hetland, R.D., DiMarco, S.F.: How does the character of oxygen demand control the structure of
 820 hypoxia on the Texas-Louisiana continental shelf? *J. Mar. Sys.*, 70, 49-62, doi:
 821 10.1016/j.jmarsys.2007.03.002, 2008.

822 Hicks, T.L., Shamberger, K.E.F., Fitzsimmons, J.N., Jensen, C.C., DiMarco, S.F. Tropical
 823 cyclone-induced coastal acidification in Galveston Bay, Texas. *Commun. Earth Environ.* 3,
 824 297, doi:10.1038/s43247-022-00608-1, 2022.

825 Horner, R. R., Skupien, J. J., Livingston, E. H., and Shaver, H. E.: *Fundamentals of urban runoff*
 826 *management: Technical and institutional issues*. Terrene Institute, Washington, D.C., 1994.

827 Jarvis, B.M., Greene, R.M., Wan, Y., Lehrter, J.C., Lowe, L.L., Ko, D.S: Contiguous low
 828 oxygen waters between the continental shelf hypoxia zone and nearshore coastal waters of
 829 Louisiana, USA: interpreting 30 years of profiling data and three-dimensional ecosystem
 830 modeling. *Environ. Sci. Technol.*, 55, 4709-4719, doi: 10.1021/acs.est.0c05973, 2021.

831 Kealoha, A.K., Doyle, S.M., Shamberger, K.E.F., Sylvan, J.B., Hetland, R.D., DiMarco, S.F.:
 832 Localized hypoxia may have caused coral reef mortality at the Flower Garden Banks. *Coral*
 833 *Reefs*, 39, 119-132, doi: 10.1007/s00338-019-01883-9, 2020.

834 Lewin, J.C. : The dissolution of silica from diatom walls. *Geochem. Cosmochim. Acta* 21, 182-
 835 198.

836 Liu, B., D'Sa, E., Joashi, I.: Floodwater impact on Galveston Bay phytoplankton taxonomy,
 837 pigment composition and photo-physiological state following Hurricane Harvey from field
 838 and ocean color (Sentinel-3A OLCI) observations. *Biogeosciences*, 16, 1975-2001;
 839 doi:10.5194/bg-2018-504, 2019.

840 Mallin, M.A., Corbett, C.A.: How hurricane attributes determine the extent of environmental
 841 effects: multiple hurricanes and different coastal systems. *Estuar. Coasts.*, 29, 1046-1061,
 842 doi: 10.1007/BF02798667, 2006.

843 Manzello, D., Enochs, I., Musielewicz, S., Carlton, R., Gledhill, D. Tropical cyclones cause
 844 CaCO₃ undersaturation of coral reef seawater in a high-CO₂ world. *J. Geophys. Res. Oceans*
 845 118, 5312-5321, 2013.

846 Montagna, P., Hu, X., Walker, L., Wetz, M. 2017. Biogeochemical impact of Hurricane Harvey
 847 on Texas coastal lagoons. AGU Fall Meeting Abstract #NH23E-2797.

848 Nowlin, W.D.Jr., Jochens, A.E., Reid, R.O., DiMarco, S.F. 1998. Texas-Louisiana Shelf
 849 Circulation and Transport Processes Study: Synthesis Report. *PCS Study MMS 98-0035*. U.S.
 850 Department of the Interior, Minerals Management Service, Gulf of Mexico OCS Region,
 851 New Orleans, LA.

852 Paerl, H.W., Bales, J.D., Ausley, L.W., Buzzelli, C.P., Crowder, L.B., Eby, L.A., Fear, J.M., Go,
 853 M., Peierls, B.L., Richardson, T.L., Ramus, J.S.: Ecosystem impacts of three sequential
 854 hurricanes (Dennis, Floyd, and Irene) on the United States' largest lagoonal estuary,
 855 Pamlico Sound, NC. *Proc. Natl. Acad. Sci. U.S.A.*, 98, 5655–5660, doi:
 856 10.1073/pnas.101097398, 2001.

857 Paerl, H.W., Crosswell, J.R., Van Dam, B., Hall, N.S., Rossignol, K.L., Osburn, C.L., Hounshell,
 858 A.G., Sloup, R.S., Harding, L.W. Jr.: Two decades of tropical cyclone impacts on North
 859 Carolina's estuarine carbon, nutrient and phytoplankton dynamics: implications for
 860 biogeochemical cycling and water quality in a stormier world. *Biogeochemistry*, doi:
 861 10.1007/s10533-018-0438-x, 2018.

862 Paerl, H.W., Valdes, L.M., Joyner, A.R., Peierls, B.L., Piehler, M.F., Riggs, S.R., Christian,
 863 R.R., Eby, L.A., Crowder, L.B., Ramus, J.S., Clesceri, E.J., Buzzelli, C.P., Luettich, R.A.:
 864 Ecological response to hurricane events in the Pamlico Sound system, North Carolina, and
 865 implications for assessment and management in a regime of increased frequency. *Estuar.*
 866 *Coasts*, 29, 1033–1045, doi:10.1007/BF02798666, 2006.

867 Peierls, B.L., Christian, R.R., Paerl, H.W.: Water quality and phytoplankton as indicators of
 868 hurricane impacts on a large estuarine system. *Estuaries*, 26, 1329-1343, doi:
 869 10.1007/BF02803635, 2003.

870 Pokryfki, L., Randall, R.E.: Nearshore hypoxia in the bottom water of the northwestern Gulf of
 871 Mexico from 1981 to 1984. *Mar. Environ. Res.*, 22, 75-90, doi: 10.1016/0141-
 872 1136(87)90081-X, 1987.

873 Potter, H., DiMarco, S.F., Knap, A.H.: Tropical cyclone heat potential and the rapid
 874 intensification of hurricane Harvey in the Texas Bight. *J. Geophys. Res. (Oceans)*, 124,
 875 2440-2451, doi:10.1029/2018JC014776, 2019.

876 Quigg, A., Sylvan, S.B., Gustafson, A.B., Fisher, T.R., Oliver, R.L., Tozzi, S., Ammerman, J.W.:
 877 Going West: nutrient limitation of primary production in the northern Gulf of Mexico and the
 878 importance of the Atchafalaya River. *Aq. Geochem.*, 17, 519-544, doi: 10.1007/s10498-011-
 879 9134-3, 2011.

880 Rabalais, N.N., Turner, R.E., Justic, D., Dortch, Q., Wiseman, W.J., Jr.: Characterization of
 881 Hypoxia: Topic 1 Report for the Integrated Assessment of Hypoxia in the Gulf of Mexico.
 882 NOAA Coastal Ocean Program Decision Analysis Series No. 15. NOAA Coastal Ocean
 883 Program, Silver Spring, Maryland, 1999.

884 Rabalais, N.N., Turner, R.E., Sen Gupta, B.K., Boesch, D.F., Chapman, P., Murrell, M.C.:
 885 Hypoxia in the northern Gulf of Mexico: Does the science support the plan to reduce,
 886 mitigate and control hypoxia? *Estuar. Coasts*, 30, 753-772, doi: 10.1007/BF02841332, 2007.

887 Rayson, M.D., Gross, E.S., Hetland, R.D., Fringer, O.B.: Time scales in Galveston Bay: an
 888 unsteady estuary. *J. Geophys. Res. (Oceans)*, 121, 2268-285, doi: 10.1002/2015JC011181,
 889 2016.

890 Roman, M.R., Adolf, J.E., Bichy, J., Boicourt, W.C., Harding, L.W., Houde, E.D., Jung, S.,
 891 Kimmel, D.G., Miller, W.D., Zhang, X.: Chesapeake Bay plankton and fish abundance
 892 enhanced by Hurricane Isabel. *EOS*, 86, 261-265, doi: 10.1029/2005EO280001, 2005.

893 Sahl, L.E., Merrell, W.J., Biggs, D.C.: The influence of advection on the spatial variability of
 894 nutrient concentrations on the Texas-Louisiana continental shelf. *Cont. Shelf. Res.*, 13, 233-
 895 251; doi: 10.1016/0278-4343(93)90108-A, 1993.

896 Shiah, F.K., Chang, S.W., Kao, S.J., Gong, G.C., Liu, K.K.: Biological and hydrographical
897 responses to tropical cyclones (typhoons) in the continental shelf of the Taiwan Strait. *Cont.*
898 *Shelf. Res.*, 20, 2029-2044, doi: 10.1016/S0278-4343(00)00055-8, 2000.

899 Shim, M.J., Cai, Y., Guo, L., Shiller, A.M.: Floodplain effects on the transport of dissolved and
900 colloidal trace elements in the East Pearl River, Mississippi. *Hydrol Proc.*, 31, 1086-1099,
901 doi: 10.1002/hyp.11093, 2017.

902 Shore, A., Sims, J.A., Grimes, M., Howe-Kerr, L.I., Grupstra, C.G.B., Doyle, S.M., Stadler, L.,
903 Sylvan J.B., Shamberger, K.E.F., Davies, S.W., Santiago-Vazquez, L.Z., Correa, A.N.S.: On
904 a reef far, far away: Anthropogenic impacts following extreme storms affect sponge health
905 and bacterial communities. *Front. Mar. Sci.*, 8: 608036, doi: 10.3389/mars.2021.608036,
906 2021.

907 Solis, G.S., Powell, G.L. : Hydrography, mixing characteristics, and residence times of Gulf of
908 Mexico estuaries. In: Bianchi, T.S., Pennock, J.R., Twilley, R.R. (eds). *Biogeochemistry of*
909 *Gulf of Mexico Estuaries*, John Wiley, NY, pp. 29-61, 1999.

910 Steichen, J.L., Labonte, J.M., Windham, R., Hala, D., Kaiser, K., Setta, S., Faulkner, P.C.,
911 Bacosa, H., Yan, G., Kamalanathan, M., Quigg, A.: Microbial, physical and chemical
912 changes in Galveston Bay following an extreme flood event, Hurricane Harvey. *Front. Mar.*
913 *Sci.*, 7, 186, doi:10.3389/fmars.2020.00.00186, 2020.

914 Suess, E.: Phosphate regeneration from sediments of the Peru continental margin by dissolution
915 of fish debris. *Geochim. Cosmochim. Acta*, 45, 577-588, doi: 10.1016/0016-7037(81)90191-
916 5, 1981.

917 Sylvan, J.B., Dortch, Q., Nelson, D.M., Brown, A.F.M., Morrison, W., Ammerman, J.W.:
918 Phosphorus limits phytoplankton growth on the Louisiana shelf during the period of hypoxia
919 formation. *Environ. Sci. Tech.*, 40, 7548-7553, doi : 10.1021/es061417t, 2006.

920 Sylvan, J.B., Quigg, A., Tozzi, S., Ammerman, J.W. : Eutrophication induced phosphorus
921 limitation in the Mississippi River plume: evidence from fast repetition rate fluorometry.
922 *Limnol. Oceanogr.*, 52, 2679-2685, doi: 10.4319/lo.2007.52.6.2679, 2007.

923 Thyng, K.M., Hetland, R.D., Socolofsky, S.A., Fernando, N., Turner, E.L., Schoenbaechler, C.:
924 Hurricane Harvey caused unprecedented freshwater inflow to Galveston Bay. *Estuar. Coasts*,
925 doi:10.1007/s12237-020-00800-6, 2020.

926 Trenberth K.E., Chang L., Jacobs P., Zhang Y., Fasullo, J.: Hurricane Harvey links to ocean heat
 927 content and climate change adaptation. *Earth's Future* 6, 730-744, doi:
 928 10.1029/2018EF000825, 2018.

929 Turner R.E., Rabalais N.N., Justic D.: Gulf of Mexico Hypoxia: Alternate States and a Legacy.
 930 *Environ. Sci. Technol.*, 42, 2323–2327, doi:10.1021/es071617k, 2008.

931 Walker, L.M., Montagna, P.A., Hu, X., Wetz, M.S.: Timescales and magnitude of water quality
 932 change in three Texas estuaries induced by passage of Hurricane Harvey. *Estuar. Coasts*, 44,
 933 960-971, doi: 10.1007/s12237-020-00846-6, 2021.

934 Walker, N.D.: Wind and eddy-related shelf/slope circulation processes and coastal upwelling in
 935 the Northwestern Gulf of Mexico. In: Sturges W, Lugo-Fernandez A, editors. Circulation in
 936 the Gulf of Mexico: Observations and Models. *Geophys. Monographs* 161, American
 937 Geophysical Union, 295-313, doi:10.1029/161GM21, 2005.

938 Walker, N.D., Leben, R.R., Balasubramanian, S.: Hurricane-forced upwelling and chlorophyll *a*
 939 enhancement within cold-core cyclones in the Gulf of Mexico. *Geophys. Res. Lett.* 32,
 940 doi:10.1029/2005GL023716, 2005.

941 WHPO. 1994. *WHP Operations and Methods*. WOCE Hydrographic Office Report 91/1, as
 942 revised, WOCE Hydrographic Programme Office, Woods Hole, MA.

943 Wiseman, W.J., Rabalais, N.N., Turner, R.E., Dinnel, S.P., McNaughton, A.: Seasonal and
 944 interannual variability within the Louisiana coastal current: stratification and hypoxia. *J.*
 945 *Mar. Sys.*, 12, 237-248, doi: 10.1016/S0924-7963(96)00100-5, 1997.

946 Zhang, J.-Z., Kelbie, C.R., Fischer, C.J., Moore, L.: Hurricane Katrina induced nutrient runoff
 947 from an agricultural area to coastal waters in Biscayne Bay, Florida. *Est. Coastal Shelf Sci.*,
 948 84, 209-218, doi: 10.1016/j.ecss.2009.06.026, 2009.

949